

Measuring Loschmidt echo via Floquet engineering in superconducting circuits

Shou-Kuan Zhao(赵寿宽), Zi-Yong Ge(葛自勇), Zhong-Cheng Xiang(相忠诚), Guang-Ming Xue(薛光明),Hai-Sheng Yan(严海生), Zi-Ting Wang(王子婷), Zhan Wang(王战), Hui-Kai Xu(徐晖凯), Fei-Fan Su(宿非凡),Zhao-Hua Yang(杨钊华), He Zhang(张贺), Yu-Ran Zhang(张煜然), Xue-Yi Guo(郭学仪),Kai Xu(许凯), Ye Tian(田野), Hai-Feng Yu(于海峰), Dong-Ning Zheng(郑东宁),Heng Fan(范桁), and Shi-Ping Zhao(赵士平)
Citation: Chin. Phys. B, 2022, 31 (**3**): 030307. DOI: 10.1088/1674-1056/ac40f8
Journal homepage: http://cpb.iphy.ac.cn; http://iopscience.iop.org/cpb

What follows is a list of articles you may be interested in

Hardware for multi-superconducting qubit control and readout

Zhan Wang(王战), Hai Yu(于海), Rongli Liu(刘荣利), Xiao Ma(马骁), Xueyi Guo(郭学仪), Zhongcheng Xiang(相忠诚), Pengtao Song(宋鹏涛), Luhong Su(苏鹭红), Yirong Jin(金贻荣), and Dongning Zheng(郑东宁)
Chin. Phys. B, 2021, 30 (**11**): 110305. DOI: 10.1088/1674-1056/ac0425

Observation of the exceptional point in superconducting qubit with dissipation controlled by parametric modulation

Zhan Wang(王战), Zhongcheng Xiang(相忠诚), Tong Liu(刘桐), Xiaohui Song(宋小会), Pengtao Song(宋鹏涛), Xueyi Guo(郭学仪), Luhong Su(苏鹭红), He Zhang(张贺), Yanjing Du(杜燕京), and Dongning Zheng(郑东宁)
Chin. Phys. B, 2021, 30 (**10**): 100309. DOI: 10.1088/1674-1056/ac0520

Quantum computation and simulation with superconducting qubits

Kaiyong He(何楷泳), Xiao Geng(耿霄), Rutian Huang(黄汝田), Jianshe Liu(刘建设), and Wei Chen(陈炜)
Chin. Phys. B, 2021, 30 (**8**): 080304. DOI: 10.1088/1674-1056/ac16cf

Universal quantum control based on parametric modulation in superconducting circuits

Dan-Yu Li(李丹宇), Ji Chu(储继), Wen Zheng(郑文), Dong Lan(兰栋), Jie Zhao(赵杰), Shao-Xiong Li(李邵雄), Xin-Sheng Tan(谭新生), and Yang Yu(于扬)
Chin. Phys. B, 2021, 30 (**7**): 070308. DOI: 10.1088/1674-1056/ac01c3

Fabrication of microresonators by using photoresist developer as etchant

Shu-Qing Song(宋树清), Jian-Wen Xu(徐建文), Zhi-Kun Han(韩志坤), Xiao-Pei Yang(杨晓沛), Yu-Ting Sun(孙宇霆), Xiao-Han Wang(王晓晗), Shao-Xiong Li(李邵雄), Dong Lan(兰栋), Jie Zhao(赵杰), Xin-Sheng Tan(谭新生), and Yang Yu(于扬)
Chin. Phys. B, 2021, 30 (**6**): 060313. DOI: 10.1088/1674-1056/abf112

RAPID COMMUNICATION

Measuring Loschmidt echo via Floquet engineering in superconducting circuits

Shou-Kuan Zhao(赵寿宽)[1,2], Zi-Yong Ge(葛自勇)[1,2], Zhong-Cheng Xiang(相忠诚)[1], Guang-Ming Xue(薛光明)[3], Hai-Sheng Yan(严海生)[1,2], Zi-Ting Wang(王子婷)[1,2], Zhan Wang(王战)[1,2], Hui-Kai Xu(徐晖凯)[3], Fei-Fan Su(宿非凡)[1], Zhao-Hua Yang(杨钊华)[1,2], He Zhang(张贺)[1,2], Yu-Ran Zhang(张煜然)[4], Xue-Yi Guo(郭学仪)[1], Kai Xu(许凯)[1,5], Ye Tian(田野)[1], Hai-Feng Yu(于海峰)[3], Dong-Ning Zheng(郑东宁)[1,2,5,6], Heng Fan(范桁)[1,2,5,6], and Shi-Ping Zhao(赵士平)[1,2,5,6,†]

[1] *Beijing National Laboratory for Condensed Matter Physics, Institute of Physics, Chinese Academy of Sciences, Beijing* 100190, *China*
[2] *School of Physical Sciences, University of Chinese Academy of Sciences, Beijing* 100190, *China*
[3] *Beijing Academy of Quantum Information Sciences, Beijing* 100193, *China*
[4] *Theoretical Quantum Physics Laboratory, RIKEN Cluster for Pioneering Research, Wako-shi, Saitama* 351-0198, *Japan*
[5] *CAS Center for Excellence in Topological Quantum Computation, University of Chinese Academy of Sciences, Beijing* 100190, *China*
[6] *Songshan Lake Materials Laboratory, Dongguan* 523808, *China*

(Received 23 November 2021; revised manuscript received 2 December 2021; accepted manuscript online 8 December 2021)

The Loschmidt echo is a useful diagnostic for the perfection of quantum time-reversal process and the sensitivity of quantum evolution to small perturbations. The main challenge for measuring the Loschmidt echo is the time reversal of a quantum evolution. In this work, we demonstrate the measurement of the Loschmidt echo in a superconducting 10-qubit system using Floquet engineering and discuss the imperfection of an initial Bell-state recovery arising from the next-nearest-neighbor (NNN) coupling present in the qubit device. Our results show that the Loschmidt echo is very sensitive to small perturbations during quantum-state evolution, in contrast to the quantities like qubit population that is often considered in the time-reversal experiment. These properties may be employed for the investigation of multiqubit system concerning many-body decoherence and entanglement, etc., especially when devices with reduced or vanishing NNN coupling are used.

Keywords: superconducting qubit, quantum simulation, Loschmidt echo, Floquet engineering

PACS: 03.67.Lx, 03.67.Bg, 03.65.Ta, 85.25.Cp **DOI:** 10.1088/1674-1056/ac40f8

1. Introduction

The Loschmidt echo is a measure of the recovery of evolving quantum state when a time-reversal procedure is applied to the system, which can be used to quantify the sensitivity of quantum evolution to perturbations.[1] It is a well-known diagnostic of quantum chaos that captures the dynamical aspect in the time domain and has many applications. Suppose that an initial quantum state $|\psi_0\rangle$ evolves for time t under a Hamiltonian H_1 and another Hamiltonian H_2 is applied between t and $2t$ in order to recover $|\psi_0\rangle$. In practical situations, it is not realistic to have H_2 exactly equal to $-H_1$, which would lead to a perfect recovery of $|\psi_0\rangle$. The existing difference $\Delta H = H_2 + H_1$ between H_2 and $-H_1$ then gives rise to an imperfect recovery of the initial state.

Due to its special properties, the Loschmidt echo has been employed to quantify decoherence[2,3] and entanglement[4] in many-body systems, and has also been used recently for coined discrete-time quantum walk study.[5] In the superconducting multiqubit systems, the detection of dynamical phase transitions[6] and the characterization of time reversibility for the out-of-time-order correlator (OTOC) measurement[7] have been reported. The OTOC is a recently proposed measure of quantum information spreading and scrambling in chaotic systems, which is shown to be directly linked to the Loschmidt echo in its thermal average.[8]

One of the key challenges for experimentally measuring the Loschmidt echo is the time reversal of quantum-state evolution. In this work, we use Floquet engineering for the first time to realize the reversal process and demonstrate the measurement of the Loschmidt echo in a superconducting 10-qubit chain. Floquet engineering, using time-periodic driving, is a powerful tool for the manipulation of quantum states and the control of their dynamic processes.[9] It has been applied in superconducting circuits for implementing qubit switch,[10] qubit-state stabilization,[11] high-fidelity quantum gates,[12,13] quantum state transfer,[14] and the model of topological magnon insulators.[15] Taking the advantage of its feasibility in tuning both the magnitude and phase of the coupling between the nearest-neighbor (NN) qubits, the measurement of OTOCs and operator spreading have been demonstrated in a recent experiment.[16] Here, using the Bell state as the initial state, we experimentally study the Loschmidt echo and discuss

†Corresponding author. E-mail: spzhao@iphy.ac.cn

© 2022 Chinese Physical Society and IOP Publishing Ltd

the imperfection of the recovery arising from the coupling between the next-nearest-neighbor (NNN) qubits and the on-site interaction in the specific superconducting multiqubit Hamiltonian which are not time reversible. Our results indicate that the Loschmidt echo is very sensitive for probing small perturbations in the quantum-state evolution process, as compared to, for instance, monitoring the qubit excited populations during a time forward and backward state evolution.

2. Device information

In Fig. 1, we show the capacitively coupled chain-like 10-qubit device used in the present work. Each qubit has a microwave line for XY control and a flux bias line for Z control, and is coupled to a $\lambda/4$ readout resonator that in turn couples to a transmission line for the measurement. The measurement setup and method have been described previously.[16] The XY pulse, Z pulse, qubit-state readout, pulse sequence timing, and gate fidelity are carefully calibrated. The device parameters are listed in Table 1. The frequency of the readout resonator $f_{\rm r}$ ranges from 6.545 GHz to 6.729 GHz, while the maximum qubit frequency $f_{\rm m}$ varies between 5.097 GHz and 5.895 GHz, and $f_{\rm i}$ is the qubit frequency at the idle point. U is the qubit on-site interaction. The energy relaxation time T_1 and the dephasing time T_2^* are measured at the idle point. The NN and NNN coupling strengths $g_{j,j+1}$ and $g_{j,j+2}$ are measured at the working point of 4.35 GHz. $F_{\rm g}$ and $F_{\rm e}$ are the readout fidelities of the ground and first-excited states, respectively.

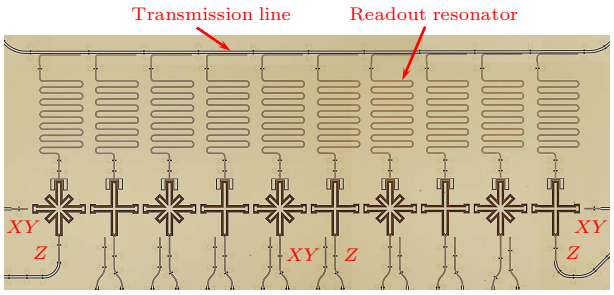


Fig. 1. Optical micrograph of the superconducting processor containing 10 transmon qubits arranged into a chain. Each qubit has a microwave line for the XY control, a flux bias line for the Z control, and a readout resonator for measurement.

Table 1. Basic device parameters. $f_{\rm r}$ is the readout resonator frequency, $f_{\rm m}$ is the qubit maximum frequency, and $f_{\rm i}$ is the qubit idle frequency. U is the qubit anharmonicity. T_1 and T_2^* are the energy relaxation time and dephasing time of the qubit at idle point, $F_{\rm g}$ and $F_{\rm e}$ are the readout fidelities for the ground and first-excited states, $g_{j,j+1}$ and $g_{j,j+2}$ are the coupling strengths of the nearest-neighbor (NN) and the next-nearest-neighbor (NNN) qubits, and δf_Φ is the detuning for the experiment with $|\Phi\rangle$ as the initial states.

	Q_1	Q_2	Q_3	Q_4	Q_5	Q_6	Q_7	Q_8	Q_9	Q_{10}
$f_{\rm r}$ (GHz)	6.545	6.563	6.587	6.609	6.630	6.648	6.642	6.689	6.709	6.729
$f_{\rm m}$ (GHz)	5.308	5.896	5.387	5.097	5.144	5.395	5.327	5.804	5.389	5.726
$f_{\rm i}$ (GHz)	4.454	5.457	4.687	5.018	4.519	5.331	4.945	5.555	5.186	4.820
$U/2\pi$ (MHz)	−212	−264	−210	−268	−212	−268	−214	−264	−214	−264
T_1 (μs)	47.6	26.3	40.4	17.5	23	29.3	46	30.8	38.2	29.3
T_2^* (μs)	1.97	2.34	1.74	6.36	2.12	36.7	2.63	3.79	3.51	1.54
$F_{\rm g}$ (%)	97.2	99.2	99.2	99.7	98.1	99.4	99.3	99.4	99.3	99.3
$F_{\rm e}$ (%)	90.4	92.6	92.4	90.7	90.3	91.7	89.9	91.7	92.5	85.6
$g_{j,j+1}/2\pi$ (MHz)	10.72	10.73	10.99	11.05	10.88	10.48	10.86	10.79	10.78	
$g_{j,j+2}/2\pi$ (MHz)		0.98	0.49	0.96	0.49	0.96	0.49	0.97	0.48	
δf_Φ (MHz)	0.950	−0.090	0.002	−0.565	−0.622	0.934	−0.869	0.563	−0.704	1.613

3. Experimental method

In the rotating frame with a common frequency, the system is governed by the 1D Bose–Hubbard model[17–19]

$$\hat{H}(t)=\sum_{j=1}^{9} g_{j,j+1}(\hat{a}_j^{\dagger}\hat{a}_{j+1}+\text{h.c.})+\sum_{j=1}^{10}\omega_j(t)\hat{n}_j+V_U+V_{\rm N}, \quad (1)$$

where

$$V_U=\sum_{j=1}^{10}\frac{U_j}{2}\hat{n}_j(\hat{n}_j-1) \text{ and } V_{\rm N}=\sum_{j=1}^{8} g_{j,j+2}(\hat{a}_j^{\dagger}\hat{a}_{j+2}+\text{h.c.})$$

are the on-site interaction and NNN coupling terms, respectively, $\hat{a}_j^{\dagger}$ ($\hat{a}_j$) is the bosonic creation (annihilation) operator, and $\hat{n}_j=\hat{a}_j^{\dagger}\hat{a}_j$ is the number operator. In our experiment, we tune the qubit frequency with ac magnetic flux to have $\omega_j(t)=\varepsilon_j\cos(\nu t)$, with ν and ε_j being the ac frequency and amplitude, respectively. The Hamiltonian $\hat{H}(t)$ thus describes a Floquet system satisfying $\hat{H}(t)=\hat{H}(t+T)$ with a period of $T=2\pi/\nu$. With $\nu\gg g_{j,j+1}$ and first neglecting V_U and $V_{\rm N}$, we obtain a time-independent Hamiltonian in spin language[9]

$$\hat{H}_{\rm eff}=\sum_{j=1}^{9} g_{j,j+1}^{\rm eff}(\hat{\sigma}_j^{+}\hat{\sigma}_{j+1}^{-}+\hat{\sigma}_{j+1}^{+}\hat{\sigma}_j^{-}), \quad (2)$$

in which $\hat{\sigma}^{\pm}=(\hat{\sigma}^x\pm \mathrm{i}\hat{\sigma}^y)/2$ with $\hat{\sigma}^{x,y,z}$ being Pauli matrices. The effective coupling strength has the form[9]

$$g_{j,j+1}^{\rm eff}\approx g_{j,j+1}\mathcal{J}_0\left(\frac{\varepsilon_j-\varepsilon_{j+1}}{\nu}\right), \quad (3)$$

where $\mathcal{J}_0(x)$ is the Bessel function of order zero.

The effective coupling strength between the NN qubits can thus be tuned by changing ε_j and $\nu/2\pi$. It follows the Bessel function which can be positive or negative leading to

a time-reversible system $\hat{H}_{\rm eff}$. In order to have a common coupling strength between each NN qubit pair, we fix $\nu/2\pi$ = 120 MHz and only drive the odd qubits with the same amplitude $|\varepsilon_j| = \varepsilon$, so the coupling strength approximates $g_j\mathcal{J}_0(\varepsilon/\nu)$. In addition, we stagger the phase of the applied flux with $\varepsilon_1, \varepsilon_5, \varepsilon_9 = \varepsilon$ and $\varepsilon_3, \varepsilon_7 = -\varepsilon$ to partly reduce the unwanted NNN coupling. In this way, we are able to set identical coupling strength for each NN qubit pair with adjustable values from positive to negative.

The Loschmidt echo now can be writen as

$$\mathcal{L}(t) = |\langle\psi_0|\, \mathrm{e}^{\mathrm{i}(\hat{H}_{\rm eff}-V_U-V_{\rm N})t}\, \mathrm{e}^{-\mathrm{i}(\hat{H}_{\rm eff}+V_U+V_{\rm N})t}\, |\psi_0\rangle|^2. \quad (4)$$

The difference between the Hamiltonians of the forward (from 0 to t) and the imperfect backward (from t to $2t$) evolution is $\Delta H = 2(V_U + V_{\rm N})$. To discuss the influence of the NNN coupling term $V_{\rm N}$, we consider the Bell state $|\Phi\rangle_{56}$ for qubits 5 and 6 while keeping the other qubits in the ground states in the 10-qubit chain:

$$|\Phi\rangle_{56} = \frac{1}{\sqrt{2}}\left(|01\rangle_{56} + \mathrm{e}^{\mathrm{i}\varphi}\,|10\rangle_{56}\right). \quad (5)$$

Since the $|\Phi\rangle_{56}$ state is the eigenstate of $\hat{N} = \sum_{j=1}^{10}\hat{n}_j$ with the number of excitations $N = 1$, the V_U term is not involved, and we can describe the system with an effective Hamiltonian $\hat{H}_{\rm eff} + V_{\rm N}$. In this work, we will consider the overlap fidelity in place of $\mathcal{L}$[7]

$$\mathcal{F}(\hat{\rho}, \hat{\rho}_0) = \left(\mathrm{Tr}\sqrt{\sqrt{\hat{\rho}}\,\hat{\rho}_0\sqrt{\hat{\rho}}}\right)^2, \quad (6)$$

in which $\hat{\rho}_0$ is the density matrix of the initial state $|\psi_0\rangle$ and $\hat{\rho}$ is that of the final state at $2t$. Here the quantity on the right-hand side of the equation is squared, as compared to the usual fidelity definition.[20] Experimental pulse sequences for the preparation of the entangled Bell state $|\Phi\rangle_{56}$ are shown in Fig. 2(a). All qubits are first biased at their idle points, and the preparation starts with the application of an X_π gate to qubit 6 followed by a $\sqrt{i\mathrm{SWAP}}$ gate between qubits 5 and 6. These operations generate an initial state of $|\Phi\rangle_{56} = (|01\rangle_{56} + \mathrm{i}\,|10\rangle_{56})/\sqrt{2}$, namely, the state in Eq. (5) with $\varphi = \pi/2$.

After the initial-state preparation, all qubits are biased to the working point for the state evolution and time-periodic driving is applied to the odd-number qubits from 0 to t and then from t to $2t$ with a staggered phase. The driving amplitude is $\varepsilon = \varepsilon_{\rm a} = 213.6$ MHz for the first period and is $\varepsilon = \varepsilon_{\rm b} = 400$ MHz for the last period. Here we have $\mathcal{J}_0(\varepsilon_{\rm a}/\nu) = -\mathcal{J}_0(\varepsilon_{\rm b}/\nu)$, corresponding to $g^{\rm eff}_{j,j+1} \approx \pm 4$ MHz for $\varepsilon_{\rm a}$ and $\varepsilon_{\rm b}$, respectively, which results in a sign change of $\hat{H}_{\rm eff}$ and the corresponding reversal of the system evolution (note we have $\nu/2\pi = 120$ MHz always). At the end of the evolution, the qubits are brought back to their idle points for the tomographic measurement, as is illustrated in Fig. 2(a).

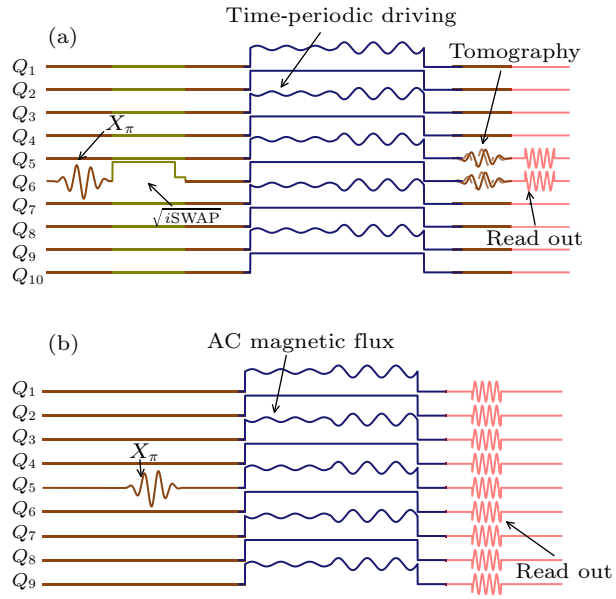


Fig. 2. (a) Pulse sequences for the 10-qubit Loschmidt echo experiment. The Bell state $|\Phi\rangle_{56}$ is first prepared for qubits 5 and 6 at their idle points with the rest of qubits remaining in the ground states. Subsequently all qubits are biased to the working point for the state evolution and time-periodic driving is applied to the odd-number qubits from 0 to t and then from t to $2t$ with different amplitude and phase. Finally, the qubits are brought back to their idle points for tomographic measurement and state readout. The orange, blue, and red pulses represent XY, Z, and readout drives, respectively. (b) Corresponding sequences for the single-photon walk and its reversed evolution experiment in the 9-qubit chain with the excitation on qubit 5.

4. Results and discussion

In the present experiment, we have set the maximum Loschmidt echo time as $t = 160$ ns. Figure 3(a) shows the density matrix representation of the experimentally measured initial Bell state $|\Phi\rangle_{56}$ prepared at time $t = 0$. As can be seen in the figure, the state is close to ideal and the overlap fidelity with the ideal $|\Phi\rangle_{56}$ state calculated with Eq. (6) is 0.97. Figure 3(b) shows the result of state tomography at $t = 80$ ns, measured with implemented qubit detuning to be discussed below. In this case, an obvious deviation from the ideal Bell state can be observed. In Fig. 4, we show our key results of the measured and calculated overlap fidelities versus the Loschmidt echo time t for the initial Bell state $|\Phi\rangle_{56}$. The circles are for the experimental data measured using the techniques and procedures described above while the dashed line is from the theoretical calculation. We find that the fidelity $\mathcal{F}$ decreases from 1 at $t = 0$ to about 0.6 at $t = 160$ ns. The clear decrease can be identified as resulting mainly from the coupling between the NNN qubits. Since we have used staggered phase of the applied flux, the NNN coupling strength between odd-number qubits has a significant reduction. For instance, when $\varepsilon/2\pi = 213.6$ MHz, we have $J_0(2\varepsilon/\nu) = -0.388$, while for $\varepsilon/2\pi = 400$ MHz, we have $J_0(2\varepsilon/\nu) = 0.282$.[16] As a result, the NNN coupling strength for all qubits is below 0.5 MHz (see Table 1).

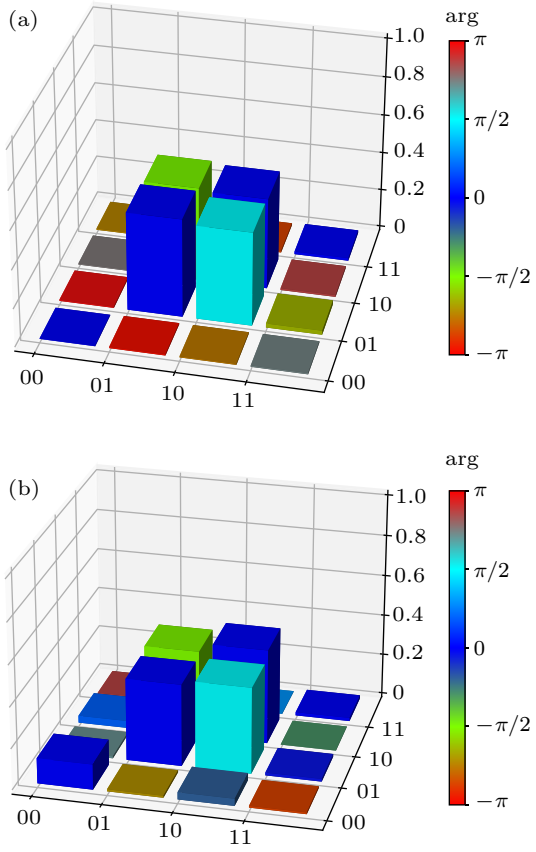


Fig. 3. Density matrix representations of the experimentally measured Bell state $|\Phi\rangle_{56}$ for the time of (a) $t = 0$ and (b) $t = 80$ ns in the Loschmidt echo experiment with qubit detuning.

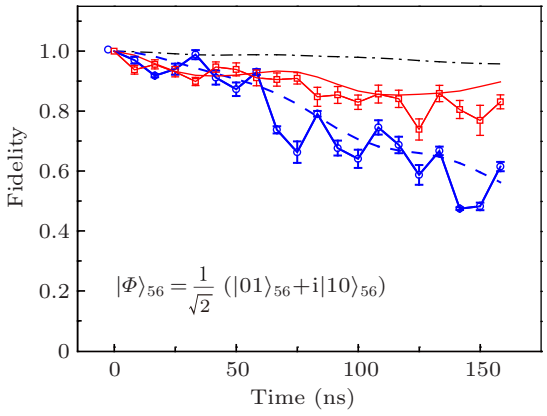


Fig. 4. Overlap fidelity defined in Eq. (6) versus Loschmidt echo time t for the initial state $|\Phi\rangle_{56}$. Thick solid and dashed lines represent the calculated results considering NNN couplings with and without qubit detuning, respectively. The squares and circles are the corresponding experimental data. The dash-dotted line is the numerical result without considering the NNN coupling.

These results indicate that the NNN coupling of small magnitude can lead to a significant decrease of the overlap fidelity. In order to see the influence further, we reduce the NNN coupling by introducing the qubit detuning quantified in the following way. In Fig. 5(a), we show the numerical results of the qubit populations at the end of the experiment shown in Fig. 2(a) with extended Loschmidt time $t = 250$ ns and considering NN and NNN coupling strengths given in Table 1. The time step is taken to be 250/30 ns. We average the populations in the time period from 125 ns to 250 ns for each qubit. The value is then maximized by adjusting the frequency detuning δf_Φ within a range of ± 2 MHz for all qubits simultaneously via the Nelder–Mead algorithm to obtain the optimized detuning δf_Φ. The final detuning δf_Φ is listed in the last row of Table 1. Figure 5(b) shows the result calculated by taking the detuning into account. In this case, the population leakage from qubits Q_5 and Q_6 to other qubits is largely suppressed.

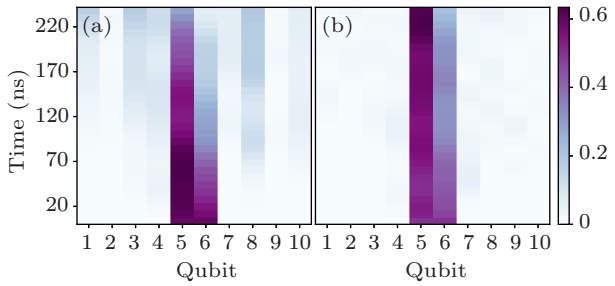


Fig. 5. Calculated population distribution versus Loschmidt echo time t for the initial state $|\Phi\rangle_{56}$. (a) Consider NN and NNN coupling strengths given in Table 1. (b) Further consider the optimized qubit frequency detuning δf_Φ in Table 1 to partially cancel the NNN coupling.

The squares and solid line in Fig. 4 are for the experimental and numerical results obtained by considering the qubit frequency detuning. We can see that the overlap fidelity has a significant increase compared to the data without considering the detuning, although it is still smaller than the result calculated without the NNN coupling, as shown in Fig. 4 with a dash-dotted line. The latter result without any NNN coupling only slightly deviates from unity with a fidelity above 0.97 at the end of $t = 160$ ns, which is attributed to the approximation taken in the derivation of the effective Hamiltonian Eq. (2) under time-periodic driving. Apparently, qubit detuning partly reduces the remaining NNN coupling and also introduces small nonuniformity of the qubit working point during the quantum-state evolution.

We point out that the Loschmidt echo is extremely sensitive to small perturbations during the quantum-state evolution, as compared, for instance, to the qubit excited populations. In Fig. 6, we show the results of the single-photon quantum walk from $t = 0$ to 125 ns, and its time-reversed evolution from $t = 125$ ns to 250 ns. The experiment is performed on a selected 9-qubit chain with the central Q_5 excited to the $|1\rangle$ state at $t = 0$. The measurement process is similar to those described above and is illustrated in Fig. 2(b). The squares in Fig. 6 are for the experimental data while the dashed and solid lines are for those calculated with and without considering the qubit NNN coupling, respectively. From the data of Q_5 calculated with NNN coupling in the figure, we find the ratio of the qubit population at $t = 250$ ns to its initial value at $t = 0$ ns to be 0.91, which is much higher than the corresponding Loschmidt echo fidelity of 0.66 at $t = 125$ ns (see the dashed line in Fig. 4). This is due to the fact that

the qubit population only reflects the norm of its excited-state wave function, whereas the phases of the wave functions are also involved in the Loschmidt echo experiment in addition to their norms.

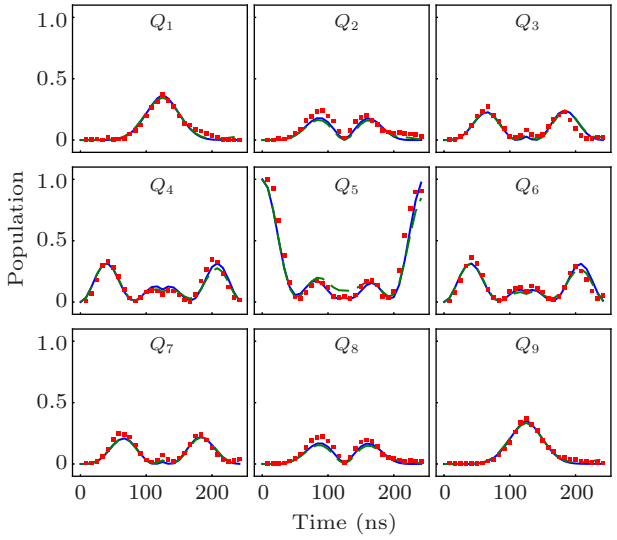


Fig. 6. Qubit populations versus time for single-photon walk and its reversed time evolution starting at $t = 125$ ns in the 9-qubit chain with the excitation on qubit 5. Symbols are the experimental results, dashed and solid lines are those calculated with and without considering the qubit NNN coupling, respectively.

Our experimental results described so far are obtained with the initial states having single-photon excitation, where the on-site interaction term V_U in the Hamiltonian can be neglected. We find that the time reversed process appears quite satisfactory if one looks at the time forward and backward evolution from the viewpoint of the qubit populations. The NNN term does not seem to show an important role in this case. The situation will be different for the initial states with multiphoton excitations. In our previous studies of OTOC in a 10-qubit chain, the recovery of the initial states is found less satisfactory when the qubit populations are monitored.[16]

5. Summary

We have successfully performed the Loschmidt echo experiment in a superconducting 10-qubit system using Floquet engineering and discussed the imperfect recovery of the initial Bell state arising from the NNN coupling present in the qubit device. Our results demonstrated that the Loschmidt echo is very sensitive to small perturbations during quantum-state forward and backward evolution. Further calculations indicate that the change of the Bell state itself such as the phase φ in Eq. (5) will also have a strong influence on the overlap fidelity. These properties may be employed for the investigation of the multiqubit system concerning many-body decoherence and entanglement, etc., especially when devices with reduced or vanishing NNN coupling between qubits are used.

Acknowledgments

This work was supported in part by the Key-Area Research and Development Program of Guang-Dong Province, China (Grant No. 2018B030326001) and the National Key R&D Program of China (Grant No. 2017YFA0304300). Y. R. Z. was supported by the Japan Society for the Promotion of Science (JSPS) (Postdoctoral Fellowship via Grant No. P19326, and KAKENHI via Grant No. JP19F19326). H. Y. acknowledges support from the Natural Science Foundation of Beijing, China (Grant No. Z190012) and the National Natural Science Foundation of of China (Grant No. 11890704). H. F. acknowledges support from the National Natural Science Foundation of China (Grant No. T2121001), Strategic Priority Research Program of Chinese Academy of Sciences (Grant No. XDB28000000), and Beijing Natural Science Foundation, China (Grant No. Z200009).

References

[1] Gorin T, Prosen T, Seligman T H and Žnidarič M 2006 *Phys. Rep.* **435** 33

[2] Jalabert R A and Pastawski H M 2001 *Phys. Rev. Lett.* **86** 2490

[3] Zangara P R, Dente A D, Levstein P R and Pastawski H M 2012 *Phys. Rev. A* **86** 012322

[4] Ho W W and Abanin D A 2017 *Phys. Rev. B* **95** 094302

[5] Omanakuttan S and Lakshminarayan A 2021 *Phys. Rev. E* **103** 012207

[6] Xu K, Sun Z H, Liu W X, Zhang Y R, Li H K, Dong H, Ren W H, Zhang P F, Nori F, Zheng D N, Fan H and Wang H 2020 *Sci. Adv.* **6** eaba4935

[7] Braumüller J, Karamlou A H, Yanay Y, Kannan B, Kim D, Kjaergaard M, Melville A, Niedzielski B M, Sung Y, Vepsäläinen A, Winik R, Yoder J L, Orlando T P, Gustavsson S, Tahan C and Oliver W D 2021 arXiv: 2102.11751 [quant-ph].

[8] Yan B, Cincio L and Zurek W H 2020 *Phys. Rev. Lett.* **124** 160603

[9] Eckardt A 2017 *Rev. Mod. Phys.* **89** 011004

[10] Wu Y, Yang L, Gong M, Zheng Y, Deng H, Yan Z, Zhao Y, Huang K, Castellano A D, Munro W J, Nemoto K, Zheng D, Sun C P, Liu Y X, Zhu X and Lu L 2018 *npj Quantum Inf.* **4** 50

[11] Lu Y, Chakram S, Leung N, Earnest N, Naik R K, Huang Z, Groszkowski P, Kapit E, Koch J and Schuster D I 2017 *Phys. Rev. Lett.* **119** 150502

[12] Reagor M, Osborn C B, Tezak N, *et al.* 2018 *Sci. Adv.* **4** eaao3603

[13] Xu Y, Hua Z, Chen T, Pan X, Li X, Han J, Cai W, Ma Y, Wang H, Song Y P, Xue Z Y and Sun L 2020 *Phys. Rev. Lett.* **124** 230503

[14] Li X, Ma Y, Han J, Chen T, Xu Y, Cai W, Wang H, Song Y P, Xue Z Y, Yin Z Q and Sun L 2018 *Phys. Rev. Appl.* **10** 054009

[15] Cai W, Han J, Mei F, Xu Y, Ma Y, Li X, Wang H, Song Y P, Xue Z Y, Yin Z, Jia S and Sun L 2019 *Phys. Rev. Lett.* **123** 080501

[16] Zhao S K, Ge Z Y, Xiang Z C, Xue G M, Yan H S, Wang Z T, Wang Z, Xu H K, Su F F, Yang Z H, Zhang H, Zhang Y R, Guo X Y, Xu K, Tian Y, Yu H F, Zheng D N, Fan H and Zhao S P 2021 arXiv: 2108.01276 [quant-ph].

[17] Roushan P, Neill C, Tangpanitanon J, *et al.* 2017 *Science* **358** 1175

[18] Yan Z, Zhang Y R, Gong M, *et al.* 2019 *Science* **364** 753

[19] Ye Y, Ge Z Y, Wu Y, *et al.* 2019 *Phys. Rev. Lett.* **123** 050502

[20] Nielsen M A and Chuang I L 2010 *Quantum Computation and Quantum Information* (Cambridge: Cambridge University Press) p. 409